CFA/VISHNO 2016

Thermoacoustic Engines and Refrigerators

S. Garrett
Penn State University, Graduate Program in Acoustics, 201 G Applied Science Bldg.,
University Park, 16802, USA
sxg185@psu.edu

The generation of sound by heat has been documented as an "acoustical curiosity" since a Buddhist monk reported the loud tone produced by a ceremonial rice-cooker in his diary in 1568. The first qualitative explanation of such phenomena was provided by Lord Rayleigh in 1878, but it was not until the work of Nikolas Rott and his collaborators, in the 1970's, that a hydrodynamic theory was created and the term "thermoacoustics" was introduced. In the early 1980's, it was shown that the opposite effect was also possible: high-amplitude sound waves could produce useful amounts of refrigeration. This overview will briefly introduce some basic theoretical concepts, then go on to examine the development of a thermoacoustic engine created to generate high-amplitude sound from a nuclear fission-heated source, as well as several thermoacoustic refrigerators. Development of these devices created new challenges related to the design of heat exchangers for acoustically-oscillatory gas flows and high-powered electrodynamic sound sources capable of producing several kilowatts of acoustic power at electroacoustic efficiencies as high as 90%. Progress toward the development of practical devices has been greatly enhanced by Los Alamos National Laboratory's development of DELTAEC, a freely-accessible, sophisticated, and user-friendly, software package.

1 Introduction

The generation of sound by heat has been documented as an "acoustical curiosity" since a Buddhist monk reported the loud tone radiated by a ceremonial rice-cooker in his diary, in 1568. [1] In 1850, Karl Friedrich Julius Sondhauss investigated an observation made by glassblowers who noticed that when a hot glass bulb was attached to a cool glass tubular stem, the stem tip sometimes emitted sound. [2] The Sondhauss tube [3] is the earliest thermoacoustic engine that is a direct antecedent of the self-powered, acoustically-telemetered sensor that will be described briefly as a modern application of this technology in the core of a nuclear reactor.

1.1 The Rayleigh criterion

The first qualitative explanation of the Sondhauss effect was provided by Lord Rayleigh [4]: "If heat be given to the air at the moment of greatest condensation or be taken from it at the moment of greatest rarefaction, the vibration is encouraged." As will be demonstrated, a standing-wave thermoacoustic engine automatically does both. The standing sound wave transfers heat from the solid substrate to the gas at the phase of the acoustic cycle during which the condensation (*i.e.*, density and pressure) is maximum and removes heat from the gas, depositing that heat on a solid substrate (at a different location), at the phase of the cycle when the condensation is a minimum.

In this process, illustrated schematically in Fig. 1, the sinusoidal variation in the gas's pressure and density at any location is replaced, to simplify the description, by a four-step articulated cycle analogous to a four-cycle automotive engine. Adjacent layers of the solid substrate are separated by several thermal penetration depths [5], δ_κ, which are approximately the length scale over which heat can diffuse during one-half of an acoustic period, $T/2 = (2f)^{-1}$.

$$\delta_\kappa = \sqrt{\frac{\kappa}{\pi \rho_m c_P f}} \,. \qquad (1)$$

The gas's thermal conductivity, mean mass density, and specific heat at constant pressure are κ, ρ_m, and c_P. For the thermoacoustic engine that will be described in Sec. 2 as an exemplary embodiment (see Fig. 2), the gas is a mixture of 25% argon and 75% helium at 2.0 MPa, with $f \cong 1{,}350$ Hz, making $\delta_\kappa \cong 50$ microns.

During the first quarter-cycle in Fig. 1, a macroscopic parcel of gas that is in thermal equilibrium with the substrate at temperature, T_o, moves toward the closest rigid end of the resonator and is compressed.

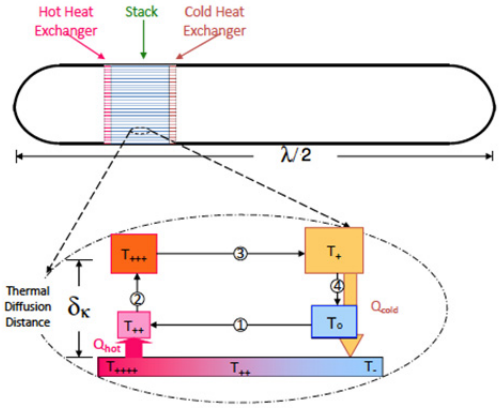

FIGURE 1 - Simplified Lagrangian representation of the thermoacoustic process that converts a temperature gradient imposed on a solid substrate (stack) to the maintenance of an acoustic standing wave in the gas contained within a half-wavelength ($\lambda/2$) long sealed resonator.

That compression is approximately adiabatic (since the gas does not have time to come to equilibrium with the substrate); hence, the increase in the parcel's temperature, δT, is related to the increase in pressure, δp. The mean gas temperature is T_m and the mean gas pressure is p_m.

$$\delta T = \left(\frac{\gamma - 1}{\gamma} \right) \frac{\delta p}{p_m} T_m \,. \qquad (2)$$

The ratio of the gas's specific heat at constant pressure to its specific heat at constant volume is $\gamma = c_P / c_V$. For an inert gas or inert gas mixture, $\gamma = 5/3$; for diatomic gases, $\gamma = 7/5$.

Conceptually, in the notation that follows, an increase in the number of '+' subscripts to the temperature, T, represents higher temperature, in arbitrary units, and the addition, or subtraction of a '++' represents the temperature increase or decrease associated with an adiabatic pressure change, as in Eq. (2). Thus, in Fig. 1, that adiabatic temperature increase, δT, is represented by the change in the parcel's temperature from T_o to T_{++}, as it moves through the first step of the articulated cycle.

During the second quarter-cycle, the gas parcel is temporarily at rest and in good thermal contact with the substrate, which is hotter than the gas. The substrate's temperature at that location is indicated as T_{++++}. Since the

parcel is cooler than the substrate, an amount of heat, Q_{hot}, flows from the substrate to the gas parcel, raising its temperature to T_{+++}, thus fulfilling the first part of Lord Rayleigh's criterion for the maintenance of the acoustic oscillation (*i.e.*, the conversion of a temperature gradient to mechanical work in the form of the standing sound wave) by adding heat "at the time of greatest condensation."

During the third quarter-cycle the gas moves away from the closest rigid end, its pressure decreased by δp, and it is cooled adiabatically, according to Eq. (2), so its temperature is decreased from T_{+++} to T_{+}. During the fourth quarter-cycle, the gas parcel is again temporarily at rest and finds itself over a portion of the substrate that is cooler, so an amount of heat, Q_{cold}, is transferred from the gas parcel at T_{+} to the substrate at T_o, thus completing the cycle and fulfilling the second part of Lord Rayleigh's criterion by removing heat "at the time of greatest rarefaction."

Typically, the stack is many acoustic displacements in overall length, and the adiabatic temperature fluctuation for a parcel of gas, per Eq. (2), is a small fraction of the mean (absolute) gas temperature, T_m. Using this Lagrangian perspective, the thermoacoustic process can be seen as a "bucket brigade" that is transferring heat from the hot end of the stack to the cooler end of the stack while doing useful work on the gas in the process. The hot heat exchanger replaces the heat on the hot end and the cold heat exchanger removes the exhaust heat (at a lower temperature) from the cold end.

It is worthwhile to point out that this is an extremely simple engine cycle when compared to an automobile engine that requires pistons, valves, cams, rocker-arms, a flywheel, etc., to have the compressions and expansions occur at the proper phases during the cycle. By contrast, this thermoacoustic process is phased by a natural process (thermal diffusion) and requires no moving parts other than the oscillatory motion of the gas. This engine is the acoustical analog of the optical laser. [6] The irreversibility of the diffusion process reduces efficiency from that achievable using a traveling-wave thermoacoustic-Stirling cycle [7], but in some applications, like the energy-rich core of a nuclear reactor, efficiency is less important than simplicity.

1.2 The critical temperature gradient

In a gas-filled resonator of length, L, that is excited in its fundamental standing-wave mode, the boundary conditions at the ends, $x = 0$ and $x = L$, require that the longitudinal gas velocity, $v_1(x, t)$, vanish, since the gas cannot pass through or deform those rigid ends. The oscillatory pressure, $p_1(x,y)$, is related to that velocity by the linearized Euler equation: $\partial\vec{v}/\partial t = -\vec{\nabla}p/\rho$.

$$v_1(x,t) = v_1 \sin\left(\frac{\pi x}{L}\right)\cos(\omega t)$$
$$p_1(x,t) = \rho_m c v_1 \cos\left(\frac{\pi x}{L}\right)\sin(\omega t) \quad (3)$$

The speed of sound in the gas is c and ρ_m is again the mean mass density of the gas. If the partial obstructions to the flow due to the stack and heat exchangers are ignored, the frequency of the first fundamental resonance, f, corresponds to one-half wavelength of the sound, $\lambda/2$, being equal to the length of the resonator: $f = \omega/2\pi = c/\lambda = c/2L$.

The displacement of a gas parcel is in time-quadrature with the gas velocity and its magnitude is given by $|x_1(x, t)| = |v_1(x, t)|/\omega$. Using the adiabatic temperature lapse of Eq. (2) and the expressions for the standing wave's oscillatory particle velocity and pressure in Eq. (3), a critical temperature gradient, $(\nabla T)_{crit}$, can be calculated as the ratio of the magnitude of the oscillating temperature, $|T_1(x, t)|$, to the magnitude of the oscillatory gas parcel displacement, $|x_1(x, t)|$.

$$(\nabla T)_{crit} \equiv \frac{|T_1(x,t)|}{|x_1(x,t)|} = 2\pi(\gamma - 1)\frac{T_m}{\lambda}\cot\left(\frac{\pi x}{L}\right) \quad (2)$$

When the temperature gradient along the stack, ∇T_m, exceeds this critical value, then the system becomes unstable and the resonant sound wave is amplified while additional heat is transported along the stack hydrodynamically by the sound wave. The amount by which ∇T_m must exceed $(\nabla T)_{crit}$ is determined by the need to overcome the ordinary thermoviscous dissipation within the resonator and the thermoacoustic components it contains (*i.e.*, the stack and heat exchanger).

Although easy to explain, this simple Lagrangian model is not well suited to the calculation of heat transport and acoustical energy production in actual thermoacoustic engines. An Eulerian formalism was developed by Nikolas Rott and co-workers who published an incredible series of papers starting in 1969. [8] Rott also introduced the term "thermoacoustics," claiming that it was self-explanatory. Rott's theoretical approach was developed further and applied to design and analysis of thermoacoustic engines and refrigerators by Greg Swift and his co-workers at the Los Alamos National Laboratory. [2,9]

2 In-Core Nuclear Fuel-Rod Sensor

A recent implementation of such a simple standing-wave thermoacoustic engine is actually even simpler than its schematic representation in Fig. 1, and simpler than more conventional standing-wave thermoacoustic engines [10], since it does not require a cold heat exchanger. The high-amplitude acoustic standing wave that is generated thermoacoustically causes the gas in the "empty" section of the resonator to be pumped by non-zero time-averaged nonlinear acoustic forces that create streaming cells. [11] This acoustically-induced flow forcibly convects heat from the ambient-temperature end of the stack to the walls of the resonator that are submerged in the reactor's cooling water. Previous measurements in a similar electrically-heated "fuel-rod resonator" have shown that this acoustically-driven streaming flow increases the thermal contact between the gas in the ambient-temperature end of the stack and the surrounding coolant by a factor-of-three. [12]

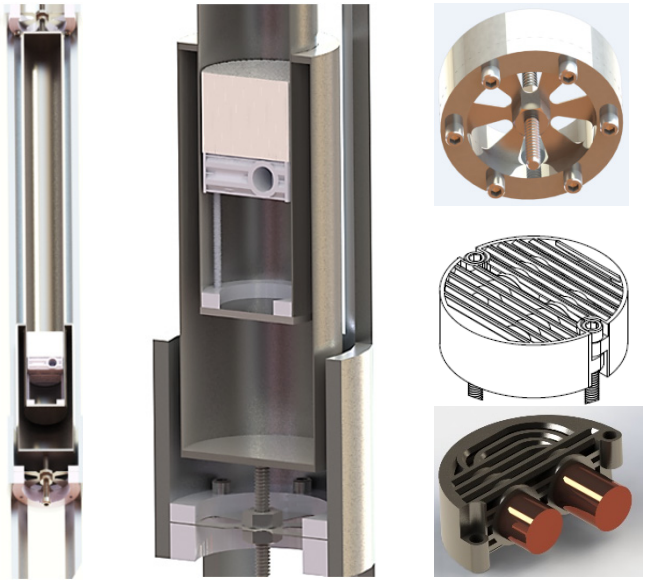

FIGURE 2 - (Left) TAC "fuel rod" sensor suspended within the "slotted tube." (Middle) Assembly cross-sectional detail showing one suspension spring and the insulation space that surrounds the resonator's hot end, hot heat exchanger, and ceramic stack. (Top Right) Suspension spring and clamp. (Middle Right) Two halves joined to make the heat exchanger. (Bottom Right) Rendering of one half of the heat exchanger with two $^{235}UO_2$ pellets installed.

This thermoacoustic sensor converts the heat released by ^{235}U fission to create a standing sound wave. It was designed to have a size and shape that is identical to the fuel rods in the Breazeale Nuclear Reactor on Penn State's University Park campus. Those fuel rods have a maximum external diameter of 3.7 cm and an overall length of 72 cm. The acoustic resonator and the "slotted tube" that contains the resonator are shown in Fig. 2 (Left). A cut-away representation of the stack, heat exchanger, suspension spring, and insulation space is shown in the central panel of Fig. 2. [13]

Based on our measurements of the vibro-acoustic spectra of the pump-dominated background noise in the coolant pool [14], a 2.0 MPa mixture of 75% helium and 25% argon was selected as the engine's "working fluid" to place the resonance frequency at about 1,350 Hz, above most of the background noise that is below 1.0 kHz. That inert gas mixture provides the largest possible polytropic coefficient (*i.e.*, ratio of specific heats) while also lowering the Prandtl number [15], thus improving the thermoacoustic energy conversion process. [16]

This thermoacoustic sensor was tested during eight irradiation runs in the Breazeale Nuclear Reactor. Provisions of the reactor's operating license limit the accumulation of radioactive iodine isotopes in the fuel pellets to less than a total of 1.5 Ci. As a consequence, the sensor's irradiation dose restricted operations to a reactor time-integrated power of approximately seven MW-minutes. Following each run, the experiment was idled while the unstable iodine isotopes were allowed to decay.

Figure 3 is one time record made during the 5th irradiation. It shows the temperature of the thermocouple that was brazed to the hot-end of the thermoacoustic resonator, contained within the insulation space, as well as the output of two hydrophones that were located far from the core in the reactor's coolant pool. Short Time Fast (essentially sliding-average) Fourier transforms of ten-second time records were produced every two seconds and the frequency of only the largest-amplitude spectral component is plotted in Fig. 3 for both hydrophones.

During the 5th irradiation, the thermoacoustic sensor achieved onset at about t = 810 s, after the start of the recording, which is the time the largest amplitude spectral components for both hydrophones coalesced to the same frequency. It is also possible to detect a subtle indication of the onset of thermoacoustic oscillations suggested by the slight increase of the slope of the thermocouple's temperature *vs*. time after onset. This increased heating rate indicated a hydrodynamically-enhanced increase in the uniformity of the distribution of the heat from the hot heat exchanger (which contains the two enriched ^{235}U fuel pellets) to all other locations within the resonator through the gas streaming. [12]

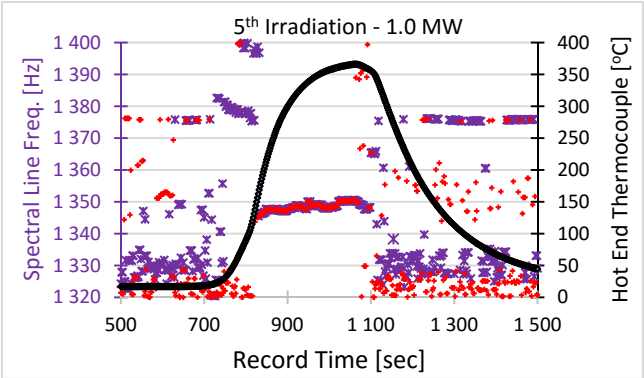

FIGURE 3 - Time record of the resonator's hot-end temperature and the frequency of the largest spectral component received by two hydrophones at two different locations in the reactor's coolant pool. The temperature of a Type-K thermocouple brazed to the hot-end of the thermoacoustic resonator is plotted as the black diamonds. The "X" and box "■" symbols are the frequencies of the largest spectral component within the frequency range between 1,320 Hz ≤ f ≤ 1,400 Hz that was recorded by the two hydrophones.

Before onset of thermoacoustic oscillations (t < 810 s) and after their cessation (t > 1,100 s), the frequencies of the dominant spectral components from both hydrophone signals are fairly random and were different due to the proximity of these hydrophones to the sources of pump noises in their respective locations. This is as would be expected when only the pump noises were received within the displayed bandwidth, Δf = ±40 Hz. The frequency of the sound determines the temperature of the reactor's coolant [17] and the amplitude determines the neutron flux. [18]

3 Merkli and Thomann's Surprise

Although thermoacoustic sound production had been observed since 1568 [1], it was not until the early-1980s that high-amplitude standing sound waves were shown to be capable of producing significant amounts of useful refrigeration. [19] In 1975, Merkli and Thomann published a result I found surprising: a high-amplitude standing wave could produce localized regions of cooling along the surface of a cylindrical standing-wave resonator that otherwise had a uniform surface temperature prior to the excitation of the standing wave. [20] I'd always

assumed that any resonator would only warm up everywhere due to the thermoviscous dissipation on its surfaces.

Unlike the case analyzed for the engine in Sec. 1.1, where a temperature gradient in excess of the critical temperature gradient of Eq. (4) is imposed, if the stack started with a uniform temperature, then the motion of the gas parcels produced by an externally-imposed standing wave would create a "bucket brigade" that moves heat from the cold heat exchanger to the hot heat exchanger. A parcel would heat adiabatically, as indicated in Eq. (2), when it moved toward the closest rigid end of the resonator in Fig. 1, then would deposit some heat on the substrate, the gas being warmer than the initially uniform-temperature substrate. The slightly cooler parcel (due to that heat loss) would then move away from the rigid end and cool adiabatically, finding itself cooler than the substrate at its new position and absorbing heat from the substrate.

3.1 A Standing-Wave Refrigerator

Figure 4 shows the cross-section of a thermoacoustic refrigerator that uses two custom-built electrodynamic loudspeakers to excite a high-amplitude, one-half wavelength, standing wave in a resonator that contains two stacks and four heat exchangers. [21]

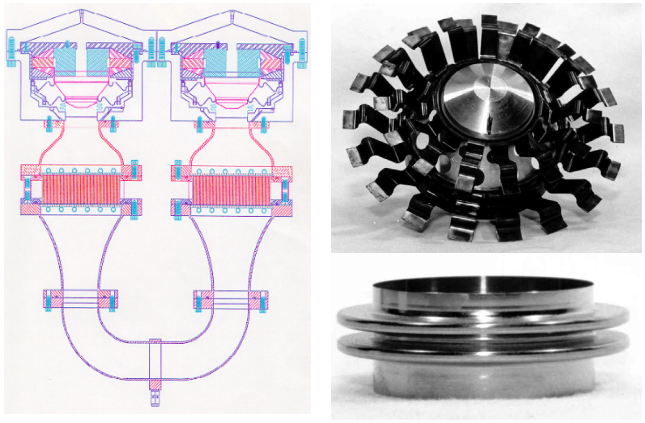

FIGURE 4 - (Left) A cross-sectional diagram of a thermoacoustic refrigerator that uses two anti-phase electrodynamic loudspeakers to excite a half-wavelength standing wave. The resonator contains two stacks. Each stack is adjacent to both a hot and a cold heat exchanger. (Upper Right) The loudspeaker's aluminum piston joins the dual suspension spring assemblies that are made from 17-7 PH stainless steel. (Lower Right) An electroformed nickel bellows provides a dynamic flexure seal between the front side of the piston and the thermoacoustic resonator.

The stacks and heat exchangers were 11.0 cm in diameter and 40.3 mm long. The stacks were constructed by rolling up 52 micron thick Kapton™ film with fishing line glued across the film every 5 mm to create uniform spacing of 280 microns when rolled into a spiral. The heat exchangers had 152 micron thick copper fins, soldered to ¼" OD copper refrigeration tubing that carried water to transport cooling and waste heat. [22] The resonator is pressurized to a mean pressure of 2.1 MPa with a mixture of 94.4% helium and 5.6% argon. The resonance frequency as around 322 ± 2 Hz.

The half-wavelength topology of this thermoacoustic refrigerator places both of the hot heat exchangers facing the loudspeakers so that any heat generated by the loudspeakers is carried off along with the mechanical work and the exhaust heat that is pumped thermoacoustically from the cold heat exchanger. Also, the two cold heat exchangers face each other through the U-shaped cold portion of the resonator that was thermally insulated to reduce nuisance heat loads from the surrounding air. The gentle bend of the resonator tube was required so that the entire system could fit inside a standard shipboard "19-inch radar rack." The changes in the resonator's cross-sectional area suppress the formation of shock waves that would dissipate additional acoustical power by production of harmonics. [23]

3.2 Coefficient-of-Performance

Just as in the case of heat engine efficiencies, the maximum coefficient-of-performance that can be achieved within the limitations imposed by the 1st and 2nd Laws of Thermodynamics, COP_{Carnot}, is determined solely by the refrigeration temperature, T_{cold}, and the exhaust temperature, T_{hot}.

$$COP_{Carnot} = \frac{T_{cold}}{T_{hot} - T_{cold}} \quad \text{and} \quad COPR = \frac{COP}{COP_{Carnot}} \qquad (3)$$

The coefficient-of-performance is the amount of useful heat per unit time (*i.e.*, cooling power), $\dot{Q}_{cold}$, moved from T_{cold} to T_{hot}, divided by power (either mechanical or electrical), Π, needed to transport $\dot{Q}_{cold}$. Since COP_{Carnot} depends upon the temperature span, $\Delta T = T_{hot} - T_{cold}$, it is convenient to express the measured coefficient-of-performance relative to the Carnot limit, *COPR*, to compare refrigerators operating over different temperature spans.

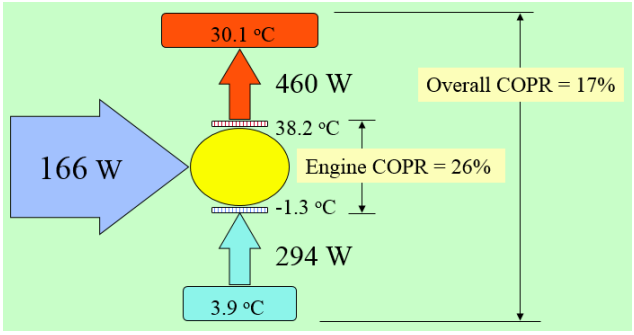

FIGURE 5 - Data taken at the coldest operating point of the thermoacoustic refrigerator shown in Fig. 4.

Figure 5 shows the results of the lowest temperature measurements made with the Shipboard Electronics ThermoAcoustic Chiller (SETAC) when it was installed on the *USS Deyo* (DD-989), where it cooled the ship's CV-2095 Radar Azimuth Converters, contained in two racks of radar electronics, for one week while underway off the coast of Virginia in April, 1995. Since the heat exchange fluids used for both the hot and cold heat exchangers were deionized water, the lowest temperature that could be achieved was limited to the freezing point of water. Based on the hot and cold stack temperatures, T_{hot} = 38.2 ºC and T_{cold} = -1.3 ºC, *COPR* = 26%. This is only slightly lower than the *COPR* for commercial domestic vapor-compress refrigerators. The actual *COPR* equals 16%, based on the more important heat exchanger fluid temperatures, T_{hot} = 30.1 ºC and T_{cold} = 3.9 ºC.

The electroacoustic efficiency of the loudspeakers which delivered Π_{ac} = 166 W of useful acoustical power to the resonator had an electroacoustic efficiency, $\eta_{el} = \Pi_{ac}/\Pi_{el}$ = 53%, so the net overall coefficient-of-performance was only $COPR_{net}$ = 8.5%. Clearly, there was quite a distance between the performance of the best thermoacoustic refrigerator and the performance of commercial vapor-compression refrigerators in 1995.

It is worthwhile to point out that the maximum electroacoustic efficiency that the electrodynamic loudspeakers designed for SETAC could achieve, based on the dimensionless Wakeland number [24], $\beta = (B\ell)^2/(R_m R_{dc}) = 87$, was η_{max} = 81%. The force produced by the current, i, through the voicecoil and magnet flux is $F = (B\ell)i$, where the voice coil's electrical resistance is R_{dc}, and the loudspeaker's mechanical resistance is R_m. The reason that the maximum value of the loudspeaker's electro-acoustic efficiency was not achieved is that it would have required the metal bellows shown in Fig. 4 (Lower Right) to undergo excursions that would have exceeded its infinite-cycle endurance limit.

It is clear that improvements had to be made to both the thermoacoustic cycle performance and to the performance of the supporting technologies, like the dynamic flexure seals [25], the loudspeakers [26], and the heat exchangers [27], if thermoacoustic technology was to become competitive.

4 Traveling-Wave Thermoacoustics

Before any of the standing-wave thermoacoustics research that has been presented, thus far, was begun, Peter Ceperley realized that the phasing of the gas velocity and the acoustic pressure required to execute the Stirling cycle [28] was identical to the pressure and velocity in an acoustic traveling wave. The experimental engine that Ceperley described in his 1979 paper used steel wool as the porous medium, called the "regenerator" (equivalent to the "stack" in a standing-wave engine). That engine did not produce any gain, but was able to demonstrate that the attenuation of the traveling wave was greater when its propagation direction went from hot to cold than when the wave propagated in the opposite direction. [29] At that time, Ceperley did not realize that the acoustical impedance of a traveling wave was too small and thus did not provide the larger pressure oscillation amplitudes associated with the smaller gas velocity amplitudes (*i.e.*, higher impedance), characteristic of a standing wave, that favored more efficient cycle performance.

Twenty years after Ceperley's first publication, at roughly the same time, Scott Backhaus and Greg Swift, at Los Alamos National Laboratory [7,30], and Kees de Blok, at Aster Thermoacoustics, in the Netherlands [31], recognized that an acoustical network could be constructed that would provide the high impedance of a standing wave and could still supply the traveling-wave phasing of gas pressure and velocity that was required to execute a Stirling cycle using sound waves instead of the traditional power piston and displacer. [28] Their insight led to the possibility of thermoacoustic engines with efficiencies as high as internal combustion engines, although to date, at a considerably lower volumetric power densities. [32]

4.1 The Lautrec Number

In the standing-wave thermoacoustic engines and refrigerator discussed previously, thermal diffusion of heat over a distance characterized by the thermal penetration depth, δ_κ, in Eq. (1), provided a "natural" mechanism for producing the necessary phasing between gas pressure and gas displacement to execute the cycle illustrated in Fig. 1. Because thermal diffusion is an irreversible process, it creates entropy that degrades the efficiency of the cycle. Only when the mean temperature gradient on the stack matches the critical gradient can the efficiency equal the Carnot maximum. Of course, this only occurs in the inviscid limit when the useful work produced by an engine or useful cooling power of the refrigerator vanishes. [33] In a Stirling cycle, the pore sizes in the regenerator, which are characterized by an hydraulic radius, r_h, are much smaller than δ_κ, so the heat transfer between the gas and the substrate occur nearly isothermally.

The dimensionless ratio of hydraulic radius, r_h, to thermal penetration depth, δ_κ, is known within the thermoacoustic community as the Lautrec number, $N_L = r_h/\delta_\kappa$. The hydraulic radius is the ratio of a pore's cross-sectional area to its perimeter. For a circular pore of radius, a, the hydraulic radius is $r_h = a/2$. For the parallel plates of the stack in Fig. 1 that are separated by $2y_o$, the hydraulic radius is half of the stack spacing, $r_h = y_o$. The porous medium is called a ''stack" if $1 \le N_L \le 5$. [34] In SETAC, N_L = 1.63. The porous medium is called a ''regenerator'' if $N_L \le 0.2$. N_L is called the Lautrec number because can indicate that your regenerator is ''too loose.'' [35]

4.2 The Thermoacoustic-Stirling Cycle

A Lagrangian picture, similar to that presented in Fig. 1, can be used to explain the thermoacoustic-Stirling cycle for the gas moving within a regenerator, where $N_L \ll 1$. In going from (a) to (c), the pressure is increasing. The gas heating during compression is transferred to the regenerator isothermally, as indicated by the **red** arrow. Going from (c) to (e), the pressure is decreasing and heat is removed from the regenerator isothermally, as indicated by the **blue** arrow.

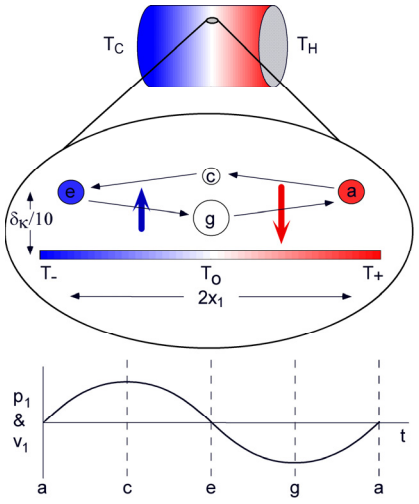

FIGURE 6 - Within the regenerator, the acoustic pressure, p_1, and the acoustic particle velocity, v_1, are in-phase. Because $N_L \ll 1$, the gas remains at nearly the same

temperature as the regenerator at every location, throughout the cycle.

Since v_1 does not change sign between (a) and (e), the gas is moving in the same direction. In going from (e) to (g), v_1 has changed sign, so the gas reverses its direction.

Going from (e) to (g) in Fig. 6, the pressure continues to decrease and again heat is removed from the regenerator and is deposited in the gas by the isothermal heat transfer indicated by the **blue** arrow. During final step in this cycle, going from (g) back to (a), the gas is being compressed and that heat of compression is transferred isothermally to the regenerator, as indicated by the **red** arrow.

The net effect is to absorb heat from the colder end of the regenerator at temperature, T_-, and deposit that heat at the warmer end of the regenerator at temperature, T_+. Since power is proportional to the product of pressure and velocity, and the pores of the regenerator are so small, it is advantageous to have gas velocities, v_1, be small and pressure changes, p_1, be large, while the traveling-wave phasing between them is maintained.

4.3 The Backhaus-Swift Engine

The first successful demonstration of an acoustic network that could provide an acoustic impedance that was favorable for acoustical execution of the Stirling cycle was achieved using the configuration shown schematically in Fig. 7. The phasing network consists of the "compliance" and "feedback inertance." These combine to produce a Helmholtz resonator that is driven at a frequency that is well below its natural Helmholtz frequency.

The Helmholtz resonator produces a pressure in the compliance that is slightly greater, by an amount, Δp_1, than the pressure at the "resonator junction" and the entrance to the "feedback inertance." That relatively small pressure difference, $\Delta p_1 \ll |p_1|$, forces gas to flow through the regenerator, which behaves as an acoustical resistance, in phase with the acoustic pressure, p_1, in the regenerator.

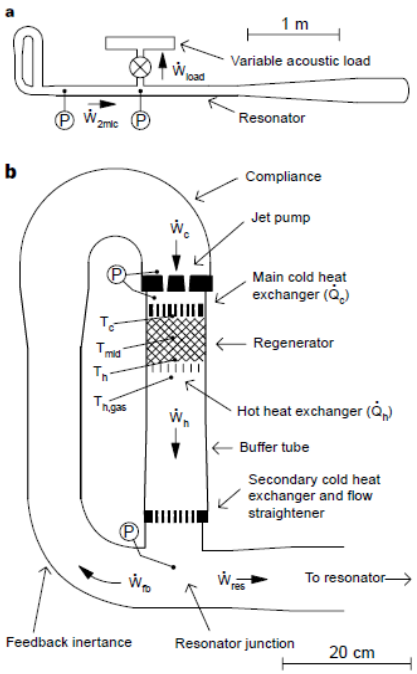

FIGURE 7 – Schematic cross-section of the Backhaus-Swift thermoacoustic-Stirling engine. The looped acoustical network that contains the regenerator, three heat exchangers, and a jet pump, shown in (b), is attached to a standing-wave resonator and a variable acoustic load. [7,30]

That loop topology allows steady circulating mass flow driven by the non-zero time-averaged product of in-phase acoustic density, ρ_1, times velocity, v_1, known as Gedeon streaming. [36] Since that mass flow also convectively transports heat, it must be suppressed. That is the function of the "jet pump" shown in Fig. 7b, which is a tapered orifice that provides a pressure difference, due to the oscillitory flow asymmetry, which was adjusted to minimize the Gedeon streaming induced thermal losses.

The Backhaus-Swift engine demonstrated an efficiency that was 30% of the Carnot limit. [7] Previous well-designed standing-wave engines that employed "natural" (*i.e.*, diffusive) phasing had efficiencies that were roughly half as large, or less. [10] For comparison, internal combustion engines have thermal efficiencies that are 25% to 40% of the Carnot limit.

4.4 The Ben & Jerry's Chiller

The first refrigerator to employ a thermoacoustic-Stirling cycle was developed for use in an ice cream sales cabinet that contained Ben & Jerry's ice cream. [27] Unlike the Backhaus-Swift heat engine, the absence of high gas temperatures allowed the Gedeon streaming to be suppressed by a loudspeaker cone that blocked dc flow while also acting as the inertance of the Helmholtz resonator, shown in Fig. 8 (Left), used to produce the pressure difference across the regenerator that would drive gas flow that was in-phase with the acoustic pressure. [37]

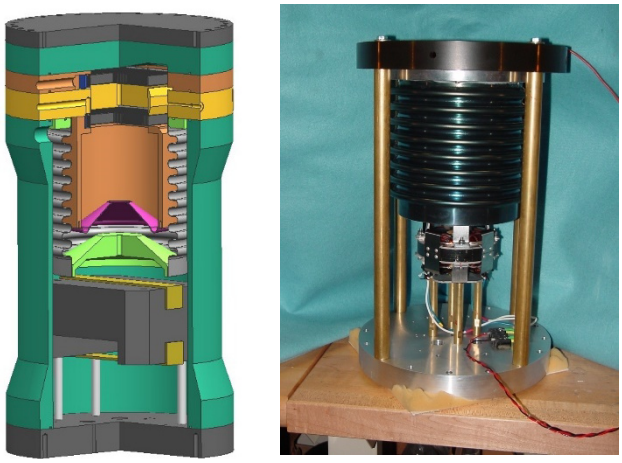

FIGURE 8 – (Left) The Ben & Jerry's chiller used a "vibromechanical multiplier" [37], consisting of the gas volume inside the orange cylinder (compliance), and the inertance (mass) provided by the loudspeaker cone (purple), as a Helmholtz resonator to produce the small pressure difference, Δp_1, that drives oscillating gas flow that is in-phase with the pressure oscillations through the regenerator (yellow) and heat exchangers (dark grey), at the top of the drawing. (Right) The oscillating pressure was created by a moving-magnet electrodynamic linear motor. [38] The moving mass of the motor and attached piston (green) resonated with stiffness of the gas within the rolled metal bellows that surrounds all of the other components.

5 Conclusion

Length restrictions limited this review of thermoacoustics to coverage of the fundamentals of standing-wave and traveling-wave thermoacoustic cycles and presentation of a few exemplary embodiments. Research continues into new configurations that improve efficiency and reduce costs with the goal of making thermoacoustics competitive with traditional engine and refrigeration technologies in the future.

Remerciements

L'auteur est reconnaissant de la gentillesse du programme HUB d'acoustique de l'Université du Maine pour soutenir ma visite annuelle au Laboratoire d'Acoustique (LAUM) et spécialement de sa collaboration avec Guillaume Penelet, Pierrick Lotton, et Gaëlle Poignand dans les domaines de la mécanique non linéaire et de thermoacoustique.

Références

[1] D. Noda and Y. Ueda, A thermoacoustic oscillator powered by vaporized water and ethanol," *Am J. Phys.* **81**(2), 124-126 (2013).

[2] G. W. Swift, Thermoacoustic engines, *J. Acoust. Soc. Am.* **84**(4), 1145-1180 (1988).

[3] C. Sondhauss, Über die Schallschwingungen der Luft in erhitzten Glasröhren und in geteckten Pfeifen von ungleicher Weite, *Ann. Phys. (Leipzig)* **79**, 1 (1850).

[4] J. W. Strutt (Lord Rayleigh), The explanation of certain acoustical phenomena, *Nature* **18**, 319-321 (1878).

[5] See §I.A. in Ref [2].

[6] S. L. Garrett and S. Backhaus, The power of sound, *American Scientist* **88**(6), 516-525 (2000); Le son transformé en froid, *Pour la Science*, Dossier N° 32, 112-117 (Juil/Oct 2001).

[7] S. Backhaus and G. W. Swift, A thermoacoustic-Stirling engine, *Nature* **399**, 335-338 (1999).

[8] N. Rott, Damped and thermally-driven acoustic oscillations in wide and narrow tubes, *Z. Angew. Math. Phys.* **26**, 230-243 (1969).

[9] G. W. Swift, *Thermoacoustics: A unifying perspective for some engines and refrigerators* (Acoust. Soc. Am., 2002); ISBN 0735400652.

[10] G. W. Swift, Analysis and performance of a large thermoacoustic engine, J. Acoust. Soc. Am. **92**(3), 1551-1563 (1992).

[11] J. W. Strutt (Lord Rayleigh), On the circulation of air observed in Kundt's tubes, and on some allied acoustical problems, *Phil. Trans. Royal Soc. London* **175**, 1-21 (1883); *Scientific Papers* (Dover, 1964), Art. 108, Vol. II, pp. 239-257.

[12] R. A. Ali and S. L. Garrett, Heat transfer enhancement through thermoacoustically-driven streaming, *Proc. of Meetings on Acoustics* (POMA) **19**, 030001 (2013).

[13] S. L. Garrett, *et al.*, Fission-powered in-core thermoacoustic sensor, *Appl. Phys. Lett*., accepted for publication, Feb. 2016.

[14] J. Hrisko, S. L. Garrett, R. W. M. Smith, J. A. Smith, and V. Agarwal, The vibroacoustical environment in two nuclear reactors, *J. Acoust. Soc. Am*. **137** (2), 2198 (2015).

[15] F. W. Giacobbe, Estimation of Prandtl numbers in binary mixtures of helium and other novel gases, J. *Acoust. Soc. Am.* **96**(6), 3538-3580 (1994).

[16] See §8.1 in Ref [9].

[17] S. L. Garrett, J. A. Smith, and D. K. Kotter, Thermoacoustic enhancements for nuclear fuel rods and other high temperature applications, *Published Pat. Appl.* US 2014/0050293 A1 (Feb. 20, 2014).

[18] M. D. Heibel, R. W. Flammang, and D. M. Sumego, Thermo-acoustic nuclear power distribution measurement assembly, *Published Pat. Appl.* US 2014/0362965 A1 (Dec. 11, 2014).

[19] J. C. Wheatley, G. W. Swift, and A. Migliori, Acoustical heat pumping engine, *US Pat.* 4,398,398 (Aug. 16, 1983).

[20] P. Merkli and H. Thomann, Thermoacoustic effects in a resonant tube, *J. Fluid Mech.* **70**(1), 161-177 (1975).

[21] S. L. Garrett, High power thermoacoustic refrigerator, *US Pat.* 5,647,216 (July 15, 1997).

[22] S. L. Garrett, D. K. Perkins, and A. Gopinath, Thermoacoustic refrigerator heat exchangers: design, analysis and fabrication, in *Heat Transfer-1994*, Proc. 10th Int. Heat Trans. Conf., Vol. IV, 375-380 (1994).

[23] S. L. Garrett, R. W. M. Smith and M. E. Poese, Eliminating nonlinear acoustical effects from thermoacoustic refrigeration systems, *Proc. 17th International Symposium on Nonlinear Acoustics* (ISNA 17), pg. 407-415 (Am. Inst. Physics, 2006).

[24] R. S. Wakeland, Use of electrodynamic drivers in thermoacoustic refrigerators, *J. Acoust. Soc. Am.* **107**(2), 827-832 (2000).

[25] S. L. Garrett, Cylindrical spring with integral gas seal, *US Pat.* 6,755,027 (June 29, 2004).

[26] S. L. Garrett, R. M. Keolian and R. W. M. Smith, High-efficiency moving magnet loudspeaker, *US Pat.* 6,307,287 (Oct. 23, 2001).

[27] M. E. Poese, R. W. M. Smith, S. L. Garrett, R. van Gerwen, and P. Gosselin, Thermoacoustic refrigeration for ice cream sales, *Int. Inst. Refrigeration 6th Gustav Lorentzen Natural Working Fluids Conference*, Glasgow, UK, 1 Sept 2004.

[28] A. J. Organ, *Thermodynamics and Gas Dynamics of the Stirling Cycle Machine* (Cambridge Univ., 1992).

[29] P. H. Ceperley, A pistonless Stirling engine – The traveling wave heat engine, *J. Acoust. Soc. Am.* **66**(5), 1508-1513 (1979).

[30] S. Backhaus and G. W. Swift, A thermoacoustic-Stirling heat engine: Detailed study, *J. Acoust. Soc. Am.* **107**(6), 3148-3166 (2000).

[31] C. M. De Blok and N. A. H. J. Van Rijt, Thermo-acoustic system, *US Pat.* 6,314,740 (Nov. 13, 2001).

[32] S. L. Garrett, Reinventing the engine, *Nature* **399**, 303-305 (1999).

[33] See §I.B in Ref [2].

[34] M. E. H. Tijani, J. C. H. Zeegers, and A. T. A. M. de Waele, The optimal stack spacing for thermoacoustic refrigeration, J. Acoust. Soc. Am. **112**(1), 128-133 (2002).

[35] S. L. Garrett, Resource Letter TA-1: Thermoacoustic engines and refrigerators, *Am. J. Phys.* **72**(1), 11-17 (2004).

[36] D. Gedeon, DC gas flows in Stirling and pulse-tube cryocoolers, in *Cryocoolers 9*, R. G. Ross, ed., pp. 385-392 (Plenum, 1997).

[37] M. E. Poese, R. W. M. Smith, R. S. Wakeland, and S. L. Garrett, Bellows bounce thermoacoustic device, *US Pat.* 6,792,764 (Sept. 21, 2004).

[38] J. Liu and S. Garrett, Characterization of a small moving-magnet electrodynamic linear motor for use in a thermoacoustic refrigerator, J. Acoust. Soc. Am. **118**(4), 2289-2295 (2005).